Joint Optimal Power Source Sizing and Data Collection Trip Planning for Advanced Metering Infrastructure Enabled by Unmanned Aerial Vehicles

Haiam Shahin, Mostafa F. Shaaban, *Senior Member*, *IEEE*, Mahmoud H. Ismail, *Senior Member*, *IEEE*, Hebat-Allah M. Mourad, and Ahmed Khattab, *Senior Member*, *IEEE*

***Abstract*—The use of unmanned aerial vehicles (UAVs) in the collection of data from wireless devices, sensor nodes, and the Internet of Things (IoT) devices has recently received significant attention. In this paper, we investigate the data collection process from a set of smart meters in advanced metering infrastructure (AMI) enabled by UAVs. The objective is to minimize the total annual cost of the electric utility by jointly optimizing the number of UAVs, their power source sizing, the charging locations as well as the data collection trip planning. This is achieved while considering the energy budgets of batteries of UAVs and the required amount of collected data. The problem is formulated as a mixed-integer nonlinear programming (MINLP), which is decoupled into two sub-problems where a candidate UAV and a number of buildings are first grouped into trips via genetic algorithms (GAs), and then the optimum trip path is found using a traveling salesman problem (TSP) branch and bound algorithm. Simulation results show that the battery capacity or the number of UAVs increases as the coverage area or the density increases.**

***Index Terms*—Advanced metering infrastructure, unmanned aerial vehicle, power source sizing, trip planning, genetic algorithm.**

I. Introduction

ADVANCED metering infrastructure (AMI) is considered as a vital part of integrated power management solutions that are based on the supervisory control and data acquisition (SCADA) system. AMI incorporates electrical hardware devices such as smart meters, smart sensors, circuit breakers, switchboards, uninterruptible power supply (UPS) systems, and communication gateways, which are recognized as the most reliable performance equipment for protection, control, and measurement [1]. AMI has many advantages such as: ① improving the energy efficiency, accurate collection, and calculation; ② reporting to the customers and utilities; and ③ maximizing the electrical network reliability and availability [2], [3].

Smart meters play an important role in AMI systems. These meters measure the voltage and current analog signals, convert them to digital signals, and then transmit them to the electric utility to be monitored and stored. Although the data can be manually collected, they are prone to errors and consume more time and cost. That is why smart meters use two-way communication to transmit the data to the utility without human intervention. The two-way communication can be achieved through wires using serial and parallel communication interfaces such as Ethernet [4], modbus [5], BAC net [6], M-bus [7], and RS485 [8] or can be wirelessly transmitted using global system for mobile (GSM) communications, ad-hoc connectivity, or general packet radio services (GPRS). Smart meters can also be connected through a power line communication (PLC) system. PLC is a wired line communication and transmission system that can provide two-way data as well as power transmission.

The use of wired communications to deliver the smart meters data to the utility is subject to the limitations such as the number of nodes allowed to be simultaneously used on the line and the maximum distance between the smart meter and the utility [9]. For example, the PLC technology uses the power line to transmit small amounts of data via long distances. The transmitted data can be attenuated and interfered from nearby devices, which might cause a high rate of data loss and scalability issues [10].

Similarly, wireless communication has its own limitations including congestion in the network due to the overload of data received from the smart meters. ZigBee, which is a wireless communication technology used for automatic meter reading where power usage, data rate, complexity, and cost of deployment are low, suffers from its own limitations, which includes limited processing capabilities and memory size in addition to possible interference due to the sharing of the same transmission medium [11]. In addition, mesh networks, which could also be used for data collection from

Manuscript received: February 14, 2021; revised: September 21, 2021; accepted: December 3, 2021. Date of CrossCheck: December 3, 2021. Date of online publication: June 20, 2022.

This work is supported by project # EFRG18-GER-CEN-10 from the American University of Sharjah.

H. Shahin, M. H. Ismail, A. Khattab, and H.-A. M. Mourad are with the Department of Electronics and Communications Engineering, Faculty of Engineering, Cairo University, Giza 12613, Egypt, and M. H. Ismail is also with the Department of Electrical Engineering, American University of Sharjah, PO Box 26666, Sharjah, The United Arab Emirates (e-mail: haiamshahin@yahoo.com; mhibrahim@aus.edu; akhattab@ieee.org; hmourad.mourad@gmail.com).

M. F. Shaaban (corresponding author) is with the Department of Electrical Engineering, American University of Sharjah, PO Box 26666, Sharjah, The United Arab Emirates (e-mail: mshaaban@aus.edu; mhibrahim@aus.edu).

DOI: 10.35833/MPCE.2021.000122

smart meters, could face the issues like fading, interference, and looping [11]. This is because each smart meter is equipped with a radio module and sends its data to the neighboring meters, which, in turn, act as repeaters for delivering the data to the access point. Then, the data are transmitted to the utility. Another example is the low-range (LoRa) network technology, which consumes low power when used for data collection from smart meters. However, it suffers from spectrum interference and the need to create a new network from scratch with new signal towers, base stations, and even portable gateways [12]. Finally, using 5G technology for collecting the data from smart meters is a possibility, which avoids the problems of LoRA. However, this comes at the expense of a significantly increased cost for the utility due to the need to use a huge number of subscribe identity module (SIM) cards as well as the monthly subscription for their associated data plan.

One possible solution for the data collection problem is to use unmanned aerial vehicles (UAVs). This solution avoids many of the problems mentioned above, especially when the UAV and the smart meter communicate through a standard well-established communication protocol, e.g., Wi-Fi. When using UAVs for data collection, the size of the battery is a trade-off between the weight and the flying range. A small-capacity low-mass battery requires more data collection trips and thus more frequent recharging of the battery, which leads to a reduction in its lifetime (due to a decrease of the lifetime of lithium polymer, which is about two to three years or 300 to 500 charge cycles [13]). A larger battery capacity means that the UAV is capable of flying for a longer time and can cover longer-distance trips. At the same time, the increased weight leads to more power consumption [14]. Thus, there is a need to choose the proper number of UAVs and their proper batteries; choose the proper starting point of each UAV; and manage the trips properly.

Based on the previous discussion, the number of UAVs and their appropriate batteries pose a constraint on the time of flying and hovering, which in turn limits the number of buildings that can be visited in each trip and affects the cost. In this paper, we present a new optimization framework to achieve a joint optimal selection of the number of UAVs and their proper batteries, the starting point selection of each UAV, and the trip planning. Specifically, the objective is to meet the utility requirement of data collection within a limited period at a minimum cost.

The contributions of this work can thus be summarized as follows.

1) An optimization problem is formulated to minimize the total annual cost for the electric utility. This cost includes the capital cost of the UAVs and their batteries as well as the operational cost of the trips. The decision variables are the optimum number of UAVs jointly with their power source sizing, the optimum location of the charging pad of each UAV as well as the trip plan of optimal data collection.

2) To deal with the formulated problem, we decouple it into two sub-problems: ① a candidate UAV and a number of buildings are first grouped into trips via genetic algorithms (GAs); and ② the optimum trip path is found using a traveling salesman problem (TSP) branch and bound algorithm.

The rest of this paper is organized as follows. Section II details the related works in the literature. In Section III, we introduce the system model while in Section IV, we present the problem formulation aiming at minimizing the total annual cost for all trips. In Section V, we present the proposed approach for solving our problem. Simulation results are then presented in Section VI before this paper is finally concluded in Section VII.

II. Related Work

In this section, we first review the most relevant works in the literature related to wireless data collection techniques in AMI. Then, we review the usage of UAVs for general data collection from wireless sensor networks (WSNs). Finally, the current state of the art related to UAV usage in AMI is discussed.

Reference [15] investigates the software details of the communication gateway in an AMI system using PLC where smart meters are connected to the gateway through a LonWorks-type industrial bus and the collected data are then transmitted from the gateway to a central computer through GSM. Similarly, [16] proposes an approach for the data collection and transmission from the energy meter to the utility through a GSM network. Despite the cost saving in data transmission, the system is shown to cause the congestion in the GSM network.

A different approach based on master-slave architecture is investigated in [17] to collect the data wirelessly from the smart meters by using the low-power wireless mesh network standard 6LoWPAN, and then send it to the server using GPRS technology. Accurate billing in real time is thus achieved. A similar proposal is given in [18] where an energy-efficient and cost-efficient solution is achieved using an IEEE 802.15.4-compliant wireless network.

As mentioned earlier, one of the key UAV applications is general data collection from WSNs. In that context, some research works are more concerned with energy. For example, [19] develops a combination of GA and ant colony optimization (ACO) to find the best path for a UAV, which is used to collect the data from Internet of Things (IoT) sensors. However, this research work is limited to the energy consumption of the sensor nodes (SNs) and does not consider the energy consumption of the UAVs. A differential evolution algorithm with population size (DEVIPS) is suggested for optimizing the deployment of UAVs in [20]. The algorithm selects the number and locations of hovering points to minimize the consumed energy of UAVs. Moreover, a new approach is developed in [21] for reliable uplink communication from IoT devices to UAVs while minimizing the power transmission of devices by calculating the best path for the UAVs. Along similar lines, [22] proposes a convex suboptimal optimization and approximation by jointly optimizing the UAV path and transmission power of SNs to minimize the transmission outage probability.

Other research works in the literature focus on minimizing the UAV trip times. Specifically, [23] suggests two metaheuristic algorithms for obtaining the optimal path of the

UAV to minimize the overall time while collecting the target data. Similarly, [24] suggests two schemes to minimize the overall trip time among all UAVs by calculating the best path. The problem is solved by using a min-max multiple traveling salesmen problem. Also, the joint optimal data collection interval, speeds of UAVs, and transmit power of sensors are suggested in [25] to minimize the total flight time of UAVs. In [26], a UAV is used to collect the data from SNs via a quasi-static block-fading channel. And the SNs, wakeup schedule and UAV trajectory are optimized. The design is formulated as a mixed-integer non-convex optimization problem and solved sub-optimally by applying the successive convex optimization technique. Similar problems are tackled in [27] and [28] but considering multiple-antenna UAVs. Finally, [29] suggests a solution for collision-free, reliable, and energy-efficient communication when using UAVs as a mobile gateway to collect the data from SNs based on the LoRa WAN protocol.

As for the data collection from smart meters using UAVs, lots of research works in the literature have already investigated this idea but under different assumptions and with different goals. For example, [30] explores joint ACO with guided local search (GLS) for optimizing data collection from smart meters using UAVs to overcome collisions while sending the collected data wirelessly. However, the focus is on minimizing the packet transmission time without consideration of other factors such as the available energy of the drone's battery or the cost of the data collection. Reference [31] focuses on the usage of UAVs in urban areas. The idea of data collection from smart meters by UAVs is also proposed in [32] and [33]. Reference [32] uses the MATLAB wireless SN platform lifetime (MATSNL) prediction and simulation package to estimate the trade-off between the battery lifetime and the data transmission size. The results prove the validity of the approach, but the research work considers neither the choice of the optimal point for charging the UAVs nor the planning of the UAV path. Reference [33] discusses the usefulness of integrating an inertial navigation system (INS) and a global positioning system (GPS) in the UAVs through experimentation. Similarly, [34] studies the design of UAV trajectories and the wireless communication protocol between the UAVs and the smart meters. In this research work, the UAVs are assumed to send a broadcast beacon to the smart meters to start sending their data. The results of the proposed approach are compared with those when using traditional manual reading of the meters in Brazilian utilities. However, we consider neither the amount of data nor the optimal battery choice for the UAV in order to minimize the total cost.

Even though several related aspects such as the methods of data collection from smart meters, trip planning of the UAVs, minimization of the transmitted power, and maximization of the data collection rate have been addressed in prior research works, the total cost of operation from the electric utility's point of view has never been considered before. This is captured in the number of UAVs needed to cover the city served by the utility, their associated power source selection, and their starting point selection, which is indeed an important decision from a practical point of view. Consequently, this paper investigates the cost minimization issue through a joint optimal number of UAVs, the starting point selection, the associated battery selection, and trip planning, which is what distinguishes this paper from all the prior research works in the literature.

III. System Model

We consider a system with k UAVs, where $k \in \mathcal{D}, \mathcal{D} = \{1, 2, \ldots, D\}$, and D is the maximum number of available UAVs. Each UAV is assumed to use only one battery from a predefined set of batteries, i.e., $\mathcal{B} = \{1, 2, \ldots, B\}$, to collect the data from the smart meters, which are installed on distributed buildings in a city. The meters are assumed to belong to the set $\mathcal{N} = \{1, 2, \ldots, N\}$ as shown in Fig. 1. Assuming the distance between any UAV and the n^{th} building is d_n. The horizontal coordinate of the d^{th} UAV is denoted by $\boldsymbol{q}_d$ and that of the n^{th} building is denoted by $\boldsymbol{q}_n$. Also, it is assumed that each UAV flies at a fixed altitude H and it collects the data from the smart meters in a total of T trips, where $T \leq N$. Moreover, we assume that each smart meter should be visited once during the data collection period $\mathcal{T}$. In addition, we denote the starting point of the k^{th} UAV by s_k, which is assumed to have coordinates $\boldsymbol{q}_{s_k} \in \mathrm{R}^{2\times 1}$. The starting point is the point where charging takes place for each UAV in preparation for its next trips. It is important to note that one common starting point for all the UAVs might not be enough for them to cover the area under the jurisdiction of the utility and that is why each UAV is allowed to have a unique starting point, i.e., subscript k. Finally, we define the subset of meters allocated to UAV k as $\mathcal{N}_k = \mathcal{N} \cup \{s_k\}$.

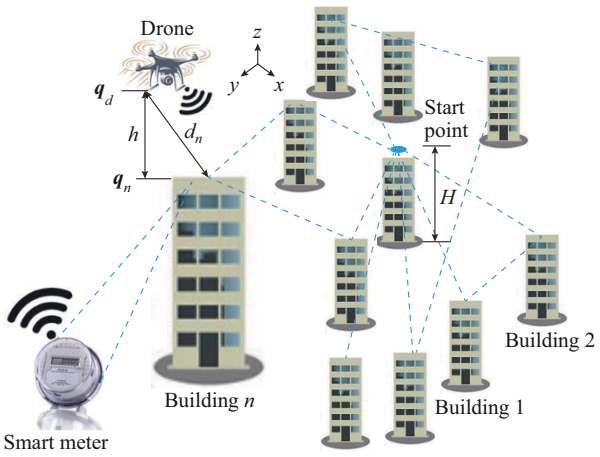

Fig. 1. Collecting data of UAVs from the smart meter.

It is assumed that the UAV can have four possible states of motion. The first is an ascending one where the UAV starts moving vertically from the ground to reach the altitude H. The second is a forwarding one where the UAV moves forward at a fixed altitude H. The third is hovering at a fixed altitude H where the UAV hovers near a building to collect the data from the smart meters. The final is a descending one from the altitude H to the ground.

As shown in Fig. 1, a UAV collects the data from a subset of buildings in each trip and the number of trips will clearly depend on the available charge in the UAV battery, the amount of target data to be collected from each smart meter, the distance between buildings as well as the number of buildings. We assume that the UAV could collect the data from each building weekly or monthly according to the utility's requirements, and the smart meters can send the data to the UAV using one of the various wireless communication technologies mentioned in [35]. It is also assumed that the link between the UAV and the smart meter during hovering is dominated by free-space line-of-sight (LOS) propagation. The LOS path loss PL_n is given by [36]:

$$PL_n = 10\alpha \lg\left(\frac{4\pi f d_n}{c}\right) + L_{los} \tag{1}$$

where α is the free-space path loss exponent; f is the carrier frequency; c is the speed of light; and L_{los} is a fixed attenuation term that is added to the LOS environment. The signal-to-noise ratio (SNR) at the UAV when communicating with the smart meter of the n^{th} building is thus expressed as:

$$SNR_n = \frac{p_n}{10^{\frac{PL_n}{10}}\sigma^2} \tag{2}$$

where p_n is the transmit power of the smart meter in building n; and σ^2 is the additive noise power.

Using Shannon's capacity formula, the achievable rate R between the UAV and a smart meter measured in bits per second can thus be obtained as:

$$R = BW \cdot \log_2\left(1 + SNR_n\right) \tag{3}$$

where BW is the allocated channel bandwidth. Finally, assuming that the amount of target data that must be collected from each smart meter is the same and is denoted by B bits, the UAV hovering time T^{HOV} during data collection from each smart meter in each building is simply given by:

$$T^{HOV} = \frac{B}{R} \tag{4}$$

IV. Problem Formulation

We aim to minimize the total annual cost of using UAVs for data collection. This includes both the capital cost of the chosen set of UAVs and their associated batteries in addition to the operation cost of all the trips per year due to the recharging of the batteries of the UAVs. This is achieved via a proper choice of the number of UAVs, their batteries as well as the proper choice of the starting points and trip planning of UAVs. The objective function of the proposed optimization problem can thus be expressed as:

$$\min_{X,Y,Z_{u,w,t,k},\mathcal{S}} \sum_{k\in\mathcal{D}} X_k\left[cost_k + \sum_{b\in\mathcal{B}} Y_{b,k}\left(cost_b + C_{b,k}^{tot}\right)\right] \tag{5}$$

where $Z_{u,w,t,k}, u, w \in \mathcal{N}_k$ and $t \in \mathcal{T} = \{1, 2, \ldots, T\}$ is another binary decision variable, which indicates that the k^{th} UAV travels from point u to w as part of trip t, and note that these points could represent actual buildings or the starting point of any UAV; X_k is a binary decision variable that indicates whether the k^{th} UAV is selected or not, and $k \in \mathcal{D}$; $Y_{b,k}$ is a binary decision variable that indicates whether battery b is associated with the k^{th} UAV, and $b \in \mathcal{B}$; $C_{b,k}^{tot}$ is the operation cost of all trips per year assuming battery b is used with the k^{th} UAV; $\mathcal{S}$ is the set of all possible points in the city, which could act as starting points for any UAV; and $cost_k$ and $cost_b$ are the annualized capital costs of the UAV and the battery, respectively. $cost_k$ is given by:

$$cost_k = CRF_k \cdot p_k \tag{6}$$

$$CRF_k = \frac{i(1+i)^{L_k^{year}}}{(1+i)^{L_k^{year}} - 1} \tag{7}$$

where p_k and CRF_k are the price and capital recovery factor (CRF) of the UAV and its associated wireless charging pad, respectively; i is the interest rate; and L_k^{year} is the lifetime of the k^{th} UAV. The CRF converts the capital cost into a series of equal annual payments that eventually pay off the UAV and its charging pad price with interest over its lifetime [37]. Also, the annualized capital cost of the battery can be calculated using the same equations in (6) and (7) but using p_b and $CRF_{b,k}$ instead. In addition, the lifetime of battery b when associated with the k^{th} UAV in years is $L_{b,k}^{year}$, which can be calculated as:

$$L_{b,k}^{year} = \min\left(\frac{L_b^{cycle}}{C_{b,k}^{cycle}}, L_{\max}\right) \tag{8}$$

where $L_{\max}$ is the chemical lifetime of any battery, which is independent of the number of recharging cycles; L_b^{cycle} is the maximum number of recharging cycles of battery b; and $C_{b,k}^{cycle}$ is the number of recharging cycles of the battery when associated with the k^{th} UAV, which is given by:

$$C_{b,k}^{cycle} = \frac{E_{b,k}^{year}}{E_b^{useful}} \tag{9}$$

where $E_{b,k}^{year}$ is the annual energy consumption, which depends on whether data collection is carried out weekly or monthly, in particular, $E_{b,k}^{year} = \mu E_{b,k}^{collection}$ with μ being the factor that captures the frequency of the data collection trips and $E_{b,k}^{collection}$ is the energy consumed for one charging cycle by the k^{th} UAV assuming battery b is installed; and E_b^{useful} is the actual useful energy of a battery, which is usually a percentage of its capacity, and specifically, $E_b^{useful} = \epsilon E_b^{max}$ with ϵ being the max depth of discharge and $E_b^{\max}$ is the battery capacity. $C_{b,k}^{tot}$ includes the expenditures related to the consumed energy during trips. This is equivalent to the cost of charging the battery and can now be calculated as:

$$C_{b,k}^{tot} = \varrho \frac{E_{b,k}^{year}}{\varphi} \tag{10}$$

where $E_{b,k}^{year}/\varphi$ is the consumed charging energy; ϱ is the price; and φ is the discharging/charging efficiency. In the following subsections, we will discuss different constraints that govern the optimization problem in (5).

A. Trip Planning Constraints

For the k^{th} UAV and for any point u that is visited in trip t, the total number of all outgoing trips to any other point needs to be equal to 1. This is necessary to ensure that every point is visited only once in all trips. Also, for any point w,

the total number of incoming trips from any other point needs to be equal to 1. Noting that these constraints do not hold for the starting point s_k, and they can be formulated respectively as:

$$\sum_{w \in \mathcal{N}_k} Z_{u,w,t,k} = 1 \quad \forall u \neq s_k, \forall t, \forall k \tag{11}$$

$$\sum_{u \in \mathcal{N}_k} Z_{u,w,t,k} = 1 \quad \forall w \neq s_k, \forall t, \forall k \tag{12}$$

In addition, to ensure that the starting point s_k for the k^{th} UAV has only one outgoing connection and only one ingoing connection during trip t, which is necessary because every feasible solution contains only one closed sequence of visited points. The following two constraints are needed.

$$\sum_{u \in \mathcal{N}_k} Z_{u,s_k,t,k} = 1 \quad \forall t, \forall k \tag{13}$$

$$\sum_{w \in \mathcal{N}_k} Z_{s_k,w,t,k} = 1 \quad \forall t, \ \forall k \tag{14}$$

Now, based on the above definitions, the total UAV flying time during trip t is equal to:

$$T_{t,k}^{fwd} = \frac{\sum_{u \in \mathcal{N}_k} \sum_{w \in \mathcal{N}_k} d_{u,w} Z_{u,w,t,k}}{V_k^{fwd}} \quad \forall t, \forall k \tag{15}$$

where V_k^{fwd} is the speed of the k^{th} UAV in the horizontal motion between any two points; and $d_{u,w}$ is the distance between points u and w, which is simply calculated as $d_{u,w} = \left\| \boldsymbol{q}_u - \boldsymbol{q}_w \right\| = \sqrt{\left(x_u - x_w\right)^2 + \left(y_u - y_w\right)^2}$, and x and y are the Cartesian coordinates and $\|\cdot\|$ indicates the Euclidean distance of a vector from the origin (2-norm). Moreover, the total hovering time of the k^{th} UAV during trip t is equal to the summation of all hovering times i.e.,

$$T_{t,k}^{hov} = T^{HOV} \sum_{u \in \mathcal{N}_k} \sum_{w \in \mathcal{N}_k} Z_{u,w,t,k} \quad \forall t, \forall k \tag{16}$$

The quantity inside the parentheses represents the total number of buildings visited in trip t by the k^{th} UAV.

Finally, observing that UAVs do not work all day long since they need time to recharge their batteries, and that utilities have specific working hours per day. The following constraint needs to be added.

$$T_{t,k}^{fwd} + T_{t,k}^{hov} \leq \tau \quad \forall k, \forall t \tag{17}$$

where τ is the maximum number of working hours per UAV.

B. Number of UAVs and Power Source Sizing Constraints of UAV

We first observe that a specific battery cannot be assigned to a certain UAV unless this UAV has already been selected to execute trips. This clearly leads to the following constraint:

$$\sum_{b \in \mathcal{B}} Y_{b,k} = X_k \quad \forall k \tag{18}$$

We also observe that since we assume only one battery will be used by the utility for each UAV, this selected battery must have a large enough capacity to cover the distance between the starting point of the selected UAV and the furthest building in the city, which leads to the following constraint:

$$\sum_{b \in \mathcal{B}} Y_{b,k} d_b^k \geq 2 d_{s_k,n} \quad \forall n \in \mathcal{N}, \forall k \tag{19}$$

where d_b^k is the maximum distance covered by the battery of the k^{th} UAV; and $d_{s_k,n}$ is the distance between the starting point of the k^{th} UAV and building n that needs to be visited and the factor 2 is needed to ensure that the UAV can come back again to its starting point for recharging.

Next, it is clear that the discharge power limit of the UAV's battery should be greater than the maximum consumed power of the battery during either hovering and data collection or forward motion, which translates into the following constraint:

$$\sum_{b \in \mathcal{B}} Y_{b,k} P_b^{\max} \geq \max\left(P_{b,k}^{hov}, P_{b,k}^{fwd}\right) \quad \forall k \tag{20}$$

where $P_b^{\max}$ is the maximum discharge rate of battery b; $P_{b,k}^{hov}$ is the power consumed during the hovering of the k^{th} UAV when powered by battery b, which depends on the mass and the velocity of the UAV; and $P_{b,k}^{fwd}$ is the power consumed during the forward movement of the k^{th} UAV. Now, the maximum discharge rate of battery b is calculated as:

$$P_b^{\max} = E_b^{\max} C_b^{rate} \tag{21}$$

$$E_b^{\max} = C_b V_b \tag{22}$$

where C_b^{rate} is the capacity rate of battery b [38]; V_b is its voltage rating; and C_b is its capacity.

$P_{b,k}^{hov}$ is calculated as:

$$P_{b,k}^{hov} = m_{b,k}^{tot} g v_{air} = m_{b,k}^{tot} g \sqrt{\frac{2 m_k^{tot}}{n_k A_k \rho}} \tag{23}$$

$$m_{b,k}^{tot} = m_{0,k} + \sum_{b \in \mathcal{B}} Y_{b,k} m_b \tag{24}$$

where $m_{b,k}^{tot}$ is the total mass of the k^{th} UAV with battery b; $m_{0,k}$ is the dead mass of the k^{th} UAV; m_b is the mass of battery b; g is the gravitational acceleration; ρ is the density of air; n_k is the number of the UAV rotors; v_{air} is the velocity of air; and A_k is the area of the cylindrical mass of air.

Finally, $P_{b,k}^{fwd}$ can be calculated as:

$$P_{b,k}^{fwd} = \frac{1}{2} \rho n_k A_k v_{air} \left(v_{air}^2 - v_{FW,b,k}^2 \sin \theta_k^2 \right) \tag{25}$$

where $v_{FW,b,k}$ is the forwarding flight velocity; and θ_k is the pitch angle [39].

$$v_{FW,b,k} = \sqrt{\frac{2 m_{b,k}^{tot} g \tan \theta_k}{\rho c_D A_k}} \tag{26}$$

where c_D is the drag coefficient depending on the geometry of the UAV. Next, the useful energy of the battery must be enough to cover each trip assuming the battery is recharged between trips. Hence, we can obtain:

$$\sum_{b \in \mathcal{B}} Y_{b,k} E_b^{useful} \geq E_{t,b,k} \quad \forall t \tag{27}$$

where $E_{t,b,k}$ is the consumed energy during trip t by using the k^{th} UAV when installing battery b, which is calculated as:

$$E_{t,b,k} = E_{t,b,k}^{fwd} + E_{t,b,k}^{hov} \tag{28}$$

where $E_{t,b,k}^{fwd}$ and $E_{t,b,k}^{hov}$ are the consumed energies by the k^{th} UAV during the forwarding and hovering motions during trip t, respectively. They are calculated as:

$$E_{t,b,k}^{fwd}=P_{b,k}^{fwd}T_{t,k}^{fwd}\quad\forall t,\ \forall k \tag{29}$$

$$E_{t,b,\ k}^{hov}=P_{b,k}^{hov}T_{t,k}^{hov}\quad\forall t,\ \forall k,\forall b \tag{30}$$

Finally, it is important to note that the total consumed energy during all trips is equal to the sum of the consumed energies during hovering and forwarding motion during all trips, which is given as follows for the k^{th} UAV.

$$E_{b,k}^{collection}=\sum_{t\in T}E_{t,b,k}^{fwd}+\sum_{t\in T}E_{t,b,k}^{hov} \tag{31}$$

Clearly, $E_{b,k}^{collection}$ can be calculated by substituting (29) and (30) into (31).

V. Proposed Approach

As explained above, the optimization problem proposed in (5) tries to jointly find the optimal number of UAVs, their associated batteries, the optimal starting point of each UAV as well as the optimal trip plan to be followed to minimize the total annual cost of the data collection process for the utility. This problem is defined as mixed-integer nonlinear programming (MINLP), which is generally complicated to find an optimal solution. Moreover, a careful look at the problem reveals that it has an embedded optimum route-selection subproblem, which is similar to the TSP whose general mathematical solution is not easy to obtain [40]. In most cases, a customized branch and bound algorithm is mostly efficient for solving a TSP. In spite of that, when using branch and bound algorithm to solve a TSP with many cities, large computational time may be required. Therefore, metaheuristic algorithms, which quickly lead to a good but not necessarily optimal solution to a TSP, are often used.

In order to solve the previously introduced MINLP optimization problem, it is decoupled into two subproblems as shown in Fig. 2. The outer subproblem is solved using GA. Inside the fitness function of the GA, we use branch and bound as a solution for the internal TSP subproblem, which becomes linear integer programming. The two subproblems are solved as follows. The outer subproblem GA selects the optimal number of UAVs, their corresponding battery sizes, the optimal starting point for each UAV, and the assigned buildings to each UAV. Moreover, the GA assigns these buildings to trips and then passes the selection to the internal branch and bound problem, which solves the TSP and calculates the optimal path for each trip. After the path calculation, the GA uses the specifications of the selected battery and path to check the constraints for each trip. Namely, the power consumption of the battery must be greater than or equal to the maximum hovering and forwarding power as well as the consumed energy must be less than or equal to the actual usable energy of the battery as shown in (20) and (27), respectively. If the constraints are not satisfied, a high penalty is assigned to the fitness function and the GA generates a new population. Finally, if the stopping criterion is met, which is chosen to be a limit on the stall generations (the number of steps the GA looks over to see whether it is making progress), the process terminates. And the output will be the optimal batteries, the trips assigned to each UAV, the buildings assigned to each trip, the optimal path for each trip, and the total annual cost for all trips.

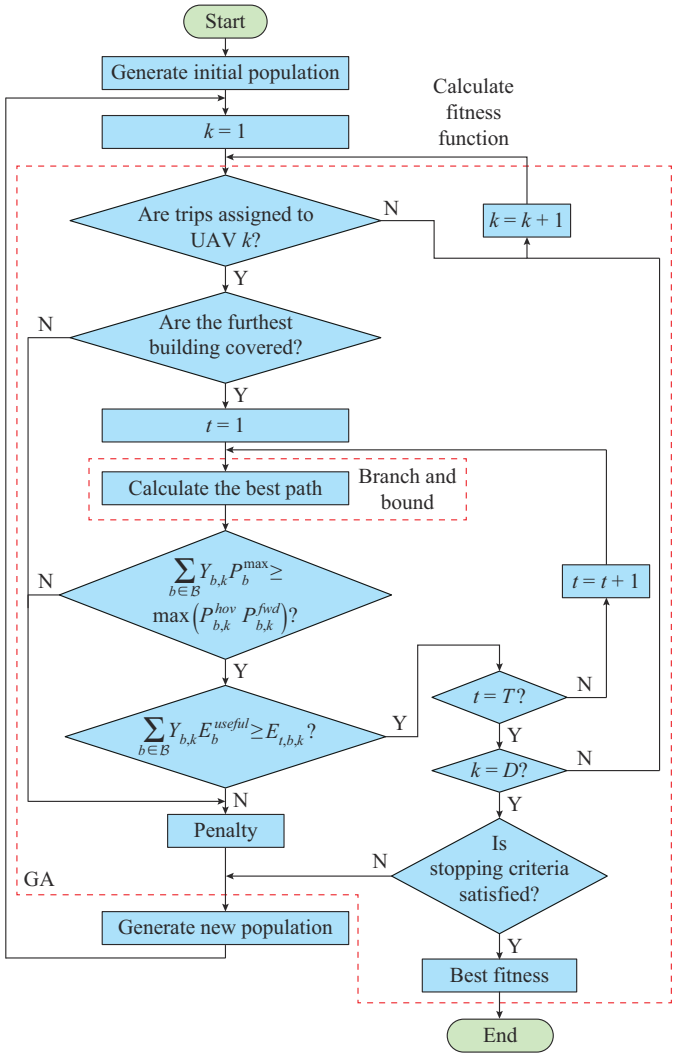

Fig. 2. Joint GA and TSP algorithms.

VI. Simulation Results and Discussions

In this section, simulation results are provided to illustrate the effectiveness of the proposed approach. We implement the approach proposed in Fig. 2 using MATLAB. The different simulation parameters are summarized in Table I.

We use the specifications of the commercial smart meter detailed in [42]. This meter stores an amount of data equals to 220 bytes per 15 min. Hence, the total amount of data stored in one smart meter per day is $D_{day}=220$ bytes × 8 bits per bytes × 4 times per hour × 24 hours per day/1024 = 165 kbits. We also assume that each building has a number of smart meters and all the meters in the building will send their data to a central server from which the UAV will be responsible for collecting the total sum of data using Wi-Fi technology. The total amount of data collected by one UAV in a trip is thus calculated as $D=D_{day}N_kN_{meters}N_{days}$, where N_k, N_{meters}, and N_{days} are the number of buildings per trip, the number of smart meters per building, and the number of days between two consecutive trips, respectively.

Furthermore, we assume that the distance between the UAV and the central server during data collection is equal for all buildings and is equal to or less than 10 meters.

TABLE I
SIMULATION PARAMETERS

Parameter	Value	Parameter	Value
BW	2.4 GHz	A_k	0.045216 m^2
H	100 m	n_k	4 rotors
V	20 km/hr	L_b^{cycle}	400
σ^2	–110 dBm	μ	52 (weekly) or 12 (monthly)
L_{los}	2 dB	φ	90%
β_0	–60 dB	$L_{\max}$	5 years
d_i	5 m	α	2.5 [41]
p_n	0.1 W	$cost_k$	\$526.7
$\mathcal{E}$	80%	L_k^{year}	5 years
ϱ	\$10^{-4}	f	910 MHz
τ	25 (weekly) or 110 (monthly)	N_{days}	7 (weekly) or 30 (monthly)
N_{meters}	50	D	1115 kbits (weekly) or 4950 kbits (monthly)
$m_{0,k}$	0.94 kg		

Regarding the candidate UAVs, for simplicity, we assume a set of 19 identical UAVs whose specifications are summarized in Table I. Also, a set of 19 batteries whose specifications are summarized in Table II is used, and the partial discharge of batteries affects their life cycles.

TABLE II
SPECIFICATIONS OF CANDIDATE BATTERIES

Battery	U (V)	C (Ah)	C_b^{rate} (h^{-1})	m_b (kg)	Price (\$)
1	11.1	350	70	0.11	8.12
2	11.1	450	70	0.12	12.18
3	11.1	1000	70	0.32	14.77
4	11.1	2200	25	0.18	15.12
5	11.1	1500	100	0.14	17.03
6	11.1	2200	25	0.41	18.62
7	11.1	2700	30	0.23	20.45
8	11.1	2200	25	0.29	20.82
9	7.4	6000	40	0.21	24.76
10	7.4	5000	50	0.20	36.50
11	11.1	7000	40	0.41	40.90
12	22.2	3200	60	0.51	48.60
13	11.1	3000	30	0.28	53.73
14	14.8	6000	50	0.59	56.70
15	22.2	5000	75	0.88	61.02
16	22.2	8000	60	1.24	85.59
17	22.2	10000	25	1.37	109.08
18	22.2	20000	25	1.50	148.64
19	22.2	22000	25	1.77	198.18

However, for lithium-ion batteries, which are assumed to be used in this paper, the so-called "memory effect" is minimal compared with other types of batteries [43]. Therefore, in this paper, we ignore this effect and assume that the partial discharge is counted as a percentage of a full cycle without affecting the battery life cycle.

For example, for the maximum depth of discharge (MDOD) of 80%, 4 cycles of 20% are counted as one full cycle. This is why in (9), we divide the total used energy in one year by the usable battery energy to calculate the number of cycles without considering whether the total annual energy is through full (the battery is empty when reaching the charging point) or partial discharge cycles.

In addition, each UAV is assumed to work for a maximum of 5 hours per day and 22 days per month or 5 days per week. This is a technical limitation on the operation of UAVs in populated areas and the flying time of UAV for each trip is still limited by its battery.

We also consider three areas for the city under investigation (1 km×1 km, 2 km×2 km, and 3 km×3 km) with four different building densities (10 buildings per km^2, 30 buildings per km^2, 50 buildings per km^2, and 100 buildings per km^2), and two cases for data collection frequency (weekly and monthly). The resulting solutions for the optimization problem in different considered cases are presented in Table III.

A. Impact of Building Density

Assuming the city area and data collection frequency are the same, increasing the building density leads to three options. The first is selecting a UAV with a high-capacity battery to increase the number of buildings per trip and consequently, decrease the number of trips. The second is to select a UAV with a low- to medium-capacity battery, which has a lower initial cost but will have a short life time and needs to be replaced in a short period. The third option is to select more than one UAV, which could cover a high building density. Clearly, the three options might require a high total annual cost. Therefore, in this paper, we use the proposed approach to select the optimal number of UAVs with proper batteries.

As shown in Table III and Fig. 3, for the case of 10 buildings per km^2 and a 1 km × 1 km city, the optimal number of trips is found to be three trips per month to collect all the required data from all smart meters, as shown in Fig. 4, and the total annual cost is about \$125.2. When the density increases to 50 buildings per km^2 for the same city area, the number of trips is found to increase to 21 trips per month, as shown in Fig. 5, and the annual cost increases to \$127.7. This is due to the fact that increasing the building density causes an increase in the amount of the consumed energy during the flying between buildings, as shown in Fig. 3. It is also observed that the UAV used in a density of 10 buildings per km^2 is not suitable for that of 50 buildings per km^2 because its battery cannot cover all buildings, so a UAV with a larger battery is needed. Also, the starting point of each UAV changes to allow the UAV to collect the target data from all buildings.

For the case of 10 buildings per km^2 and a 3 km×3 km city, only one UAV with a high-capacity battery collects the data from all buildings.

When the building density for the same city area increases to 100 buildings per km^2, using only one UAV to collect the data from all buildings is found to be infeasible. However, using the proposed approach, the optimal number of UAVs

for this case is found to be two with the following starting points: (1982, 1562) and (1905, 1906), as shown in Table III. In other words, the buildings are divided into two groups, each of which will be served by a specific UAV and will have a specific charging point. Each UAV starts its trip from its designated starting point and has to return to it after the trip finishes for re-charging. Note that, as mentioned above, these points are static and will not change for a city once picked. After a significant growth in a city, the optimization algorithm might need to be run again to find an updated number of UAVs along with their batteries and new starting points.

TABLE III
SIMULATION RESULTS

Building density (No. of buildings per km^2)	Data collection frequency	Battery used (mAh, V)	No. of trips	Starting point	Total annual cost ($)
10	Monthly	(2200, 11.1)	3	(542.6, 533)	125.2
		(6000, 7.4)	24	(879, 1251.3)	133.1
		(20000, 22.2)	20	(1618, 1247)	172.0
	Weekly	(2200, 11.1)	2	(520.5, 440.1)	125.3
		(6000, 7.4)	24	(572.5, 1147)	170.1
		(20000, 22.2)	19	(902.2, 919.5)	388.8
30	Monthly	(2200, 11.1)	12	(500, 500)	125.3
		(7000, 11.1)	66	(1000, 1000)	164.5
		(20000, 22.2)	73	(1410, 1590)	333.7
	Weekly	(6000, 7.4)	12	(500, 500)	133.5
		(7000, 11.1)	70	(964.1, 1001.3)	299.0
		(20000, 22.2)	71	(1349.1, 1650.9)	985.7
50	Monthly	(6000, 7.4)	21	(500, 500)	127.7
		(7000, 11.1)	118	(924.4, 983.1)	192.2
		(20000, 22.2)	123	(1511, 1499.8)	489.2
	Weekly	(6000, 7.4)	21	(500, 500)	143.3
		(7000, 11.1)	121	(1080, 1009.7)	416.1
		2 identical (20000, 22.2)	67, 71	(1429, 1805), (14889, 1620)	1, 957
100	Monthly	(6000, 7.4)	43	(481.9, 501.8)	133.1
		(7000, 11.1)	254	(1000, 1000)	269.3
		2 identical (20000, 22.2)	146, 141	(1982, 1562), (1905, 1906)	1, 71.7
	Weekly	(20000, 22.2)	2	(481.9, 495.3)	168.1
		(20000, 22.2)	44	(1000, 1000)	791.3
		3 identical (20000, 22.2)	99, 87, 87	(1773, 1295.6), (1656, 1791.5), (1312.3, 1304)	4, 189.5, -

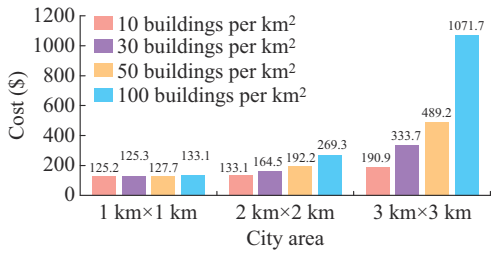

Fig. 3. Total annual cost versus area and density for monthly collection.

B. Impact of Coverage Area

For the same building density and data collection frequency, increasing the city area leads to an increase of the distances that the UAVs need to cover in order to collect the target data from buildings. Consequently, the number of trips increases, the UAV consumes more energy to cover all target buildings, and an increase in the total annual cost is expected.

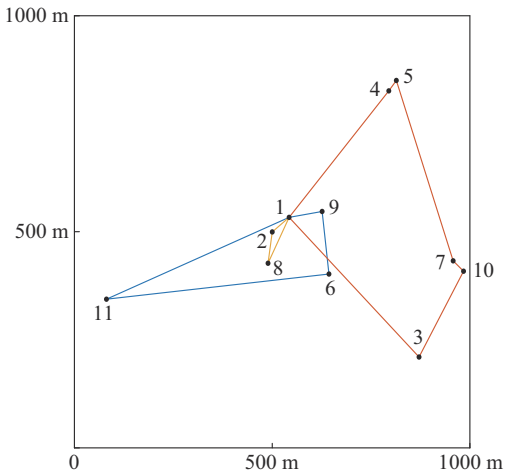

Fig. 4. Trip plan for a city with a density of 10 buildings per km^2, city area of 1 km×1 km, and monthly data collection.

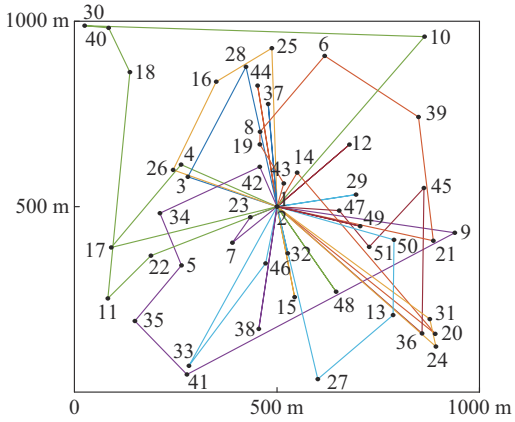

Fig. 5. Trip plan for a city with a density of 50 buildings per km^2, city area of 1 km × 1 km, and monthly data collection.

Compared with the results presented in Fig. 4 where the city area is 1 km×1 km, when the city area increases to 3 km×3 km while keeping the same building density, the number of trips increases to 20 trips per month and a UAV with a larger battery is chosen by the proposed approach. Also, the total annual cost increases to \$190.9 as shown in Table III and Fig. 3. Furthermore, compared with the results where the city area is 1 km×1 km and building density is 100 buildings per km^2, one UAV with a medium capacity battery is used. When the city area increases to 3 km × 3 km while keeping the same building density, two UAVs with larger batteries and two different starting points are chosen by the proposed approach and the total annual cost increases, as shown in Table III. This means that a city with a larger area will incur a significant increase in the cost due to higher energy consumption during the forwarding compared with the hovering.

C. Impact of Data Collection Frequency

Assuming a city area of 1 km×1 km and a density of 30 buildings per km^2, if the data collection frequency is monthly, the number of trips is found to be 12, as shown in Table III. Clearly, the algorithm selects a UAV with a small battery (2200 mAh, 11.1 V) and the cost is \$125.5, which is quite expected because the distance that the UAV needs to fly in order to reach all buildings is small. Also, the number of buildings that the UAV needs to visit and collect the data from is very few so the proposed approach chooses a UAV with a small battery that can achieve the requirements with low cost. If the data collection frequency becomes weekly, the number of trips changes to 12 trips per week (48 monthly trips). Therefore, a larger battery is selected (6000 mAh, 7.4 V) and the cost becomes \$133.5, as shown in Fig. 6. In the case of a 3 km×3 km city, the weekly data collection leads to almost a threefold increase in the cost compared with a monthly data collection, as shown in Fig. 6.

Clearly, using a UAV with a small battery for weekly data collection leads to consuming the battery quickly and results in a need to change it over a relatively short period of time and an increase in the cost. Likewise, for monthly data collection, the proposed approach does not use a UAV with a large battery.

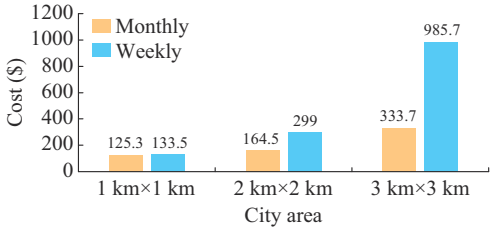

Fig. 6. Total annual cost versus data collection frequency for a density of 30 buildings per km^2.

This is because using one battery for only 12 trips per month is not an efficient and proper utilization of the battery before its chemical lifetime expires. Besides, the data collection frequency affects the number of UAVs. In the case of an area of 3 km × 3 km and a density of 50 buildings per km^2, when the data collection frequency is monthly, only one UAV collects the data from all buildings but when the data collection frequency changes to weekly, one UAV fails to collect the data from all buildings and the algorithm chooses two UAVs to cover all buildings, as shown in Table III.

D. Solution Sensitivity to Number of Runs and Type of Metaheuristic Algorithm

Since the optimal solution in this paper is obtained using a metaheuristic algorithm, which is GA, it is important to ensure its quality and check its stability across a number of simulation runs. Towards this end, we choose to repeat the simulation 100 times for the case of a city with the area of 1 km×1 km and the density of 10 buildings per km^2. For each run, the obtained optimal solution, the number of generations needed by the GA to reach the obtained optimal solution and the run time are all recorded. The results are summarized in Table IV.

TABLE IV
TOTAL ANNUAL COST OBTAINED BY EMPLOYING BOTH GA AND SIMULATED ANNEALING (SA)

Category	Total annual cost (\$)	No. of generations for GA	Run time (s)
Maximum	125.1960	305	64.990
Minimum	125.1800	124	27.778
Mean	125.1890	170	41.000
Standard deviation	0.0046	35	9.200

Clearly, the robustness of the obtained optimal solution is demonstrated since across the 100 runs, the variations in the total annual cost are minimal. Although there are considerable changes in the number of generations that the GA has to go through different run times, consequently, this doesn't affect the quality and stability of the obtained optimal solution. Furthermore, in order to check the sensitivity of the obtained optimal solution to the type of the metaheuristic algorithm used in the outer subproblem, as shown in Fig. 2, we conduct new simulation using a different optimization technique other than GA, which is SA. Table V summarizes the total annual cost obtained by employing both GA and SA.

Clearly, the new algorithm provides very close results to those obtained via GA, which confirms the stability of the proposed approach and shows that an optimum value is indeed obtained.

TABLE V
COMPARISON BETWEEN TOTAL ANNUAL COST OBTAINED USING GA AND SA

City area	Building density	Algorithm	Total annual cost ($)
1 km×1 km	10	GA	125.2
		SA	125.2
	30	GA	125.3
		SA	125.6
	50	GA	127.6
		SA	127.6
2 km×2 km	10	GA	133.1
		SA	134.2
	30	GA	164.5
		SA	164.6
	50	GA	192.2
		SA	193.0
3 km×3 km	10	GA	172.9
		SA	172.9
	30	GA	333.7
		SA	334.3
	50	GA	489.2
		SA	489.2

E. Effect of GA Parameters on Quality of Obtained Optimal Solution

As mentioned above, there is no significant difference between using GA and SA for solving the problem. We now focus on a different aspect of the proposed approach, which is the effect of the chosen GA parameters on the quality of the obtained optimal solution as described in [44]-[46].

It is clear that different configurations and combinations of the GA parameters need to be tested to judge the sensitivity of the obtained optimal solution to such variations. In this paper, the results provided so far are obtained assuming the following GA parameters: the population size is 100; the mutation, which specifies how the GA introduces small random changes in the individuals in the population to create mutation children, is done in a uniform way with a rate of 0.02; and the crossover fraction or crossover rate, which determines the fraction of the next generation produced by crossover, is set to be 0.8. In order to provide more insights, we herein investigate the obtained optimal solution for other values of these parameters.

We start by varying the population size while keeping the remaining parameters fixed, as detailed in Table VI. Clearly, increasing the population size results in a negligible improvement in the total annual cost. This improvement is obtained at the expense of a significant increase in the run time of the algorithm, which does not justify the gain obtained.

We next investigate the effect of crossover type and total annual cost as shown in Table VII.

TABLE VI
POPULATION SIZE AND TOTAL ANNUAL COST

Population size	Total annual cost ($)
50	333.985
100	333.700
150	330.828
200	329.132

TABLE VII
CROSSOVER TYPE AND TOTAL ANNUAL COST

Crossover type	Total annual cost ($)
Uniform with rate 0.8	333.700
Heuristics with rate 1.2	343.410
Heuristics with rate 1.5	346.874
Heuristics with rate 0.9	343.271
Heuristics with rate 0.5	343.322

Our initial choice to go with a uniform crossover with rate 0.8 provides the best optimal solution among the test scenarios. Finally, the effect of the mutation rate is studied in Table VIII, which also confirms that the initial choice has the minimum total annual cost among the test scenarios.

TABLE VIII
MUTATION RATE AND TOTAL ANNUAL COST

Mutation rate	Total annual cost ($)
Uniform with rate 0.01	342.779
Uniform with rate 0.02	333.700
Uniform with rate 0.03	346.854

VII. CONCLUSION

In this paper, we have studied data collection trip planning for AMI enabled by UAVs. We have formulated and solved an optimization problem where the total annual cost is minimized by jointly determining the optimal path for a trip as well as selecting the optimal number of UAVs, their associated batteries, and the optimal starting point for each UAV.

The resulting MINLP optimization problem has been solved using an iterative algorithm alternating between a GA and a branch and bound algorithm. Due to the constraints on the energy and power of a UAV, the UAV may not be able to collect the target data in one trip, so the GA groups the buildings into trips and selects the optimal number of UAVs with proper batteries and with appropriate starting points, whereas the branch and bound algorithm selects the optimal path for each trip.

Simulation results have shown the impact of the city area, density, and data collection frequency on the selection of the optimal batteries and the selection of an optimal path for each trip. Moreover, the obtained optimal solution exhibits considerable robustness against changing the different GA parameters such as the population size and crossover type. Finally, we show that the optimization problem can actually

be solved by other metaheuristic algorithms such as SA, and no significant difference in the solution quality is observed.

REFERENCES

[1] E. Kabalci and Y. Kabalci, *Smart Grids and Their Communication Systems*, Singapore: Springer Verlag, 2019.

[2] V. C. Gungor and F. C. Lambert, "A survey on communication networks for electric system automation," *Computer Networks*, vol. 50, no. 7, pp. 877-897, May 2006.

[3] R. R. Mohassel, A. Fung, F. Mohammadi *et al*., "A survey on advanced metering infrastructure," *International Journal of Electrical Power and Energy Systems*, vol. 63, pp. 473-484, Dec. 2014.

[4] *IEEE 802.3-2018*, IEEE Standard for Ethernet, 2018.

[5] M. K Vernon, E. D Lazowska, and J. Zahorjan, "An accurate and efficient performance analysis technique for multiprocessor snooping cache-consistency protocols," in *Proceedings of the 15th Annual International Symposium on Computer Architecture*, Hawaii, USA, May 1988, pp. 308-315.

[6] BACnet. (2014, Jan.). Introduction to BACnet. [Online]. Available: https://www.ccontrols.com/pdf/BACnetIntroduction.pdf

[7] P. Masek, D. Hudec, J. Krejci *et al*., "Communication capabilities of wireless m-bus: remote metering within smart grid infrastructure," in *Proceedings of International Conference on Distributed Computer and Communication Networks*, Moscow, Russia, Sept. 2018, pp. 31-42.

[8] *Electrical Characteristics of Generators and Receivers for Use in Balanced Digital Multipoint Systems*, Technical Standard TIA-485, 1998.

[9] J. H. Huh, S. Otgonchimeg, and K. Seo, "Advanced metering infrastructure design and testbed experiment using intelligent agents: focusing on the PLC network base technology for smart grid system," *Journal of Supercomputing*, vol. 72, no. 5, pp. 1862-1877, Mar. 2016.

[10] B. A. Siddiqui, P. Pakonen, and P. Verho, "Experience of communication problems in PLC-based AMR systems in Finland," in *Proceedings of 2014 IEEE PES Innovative Smart Grid Technologies Conference Europe*, Istanbul, Turkey, Oct. 2015, pp. 1- 6.

[11] S. Supriya, M. Magheshwari, S. S. Udhyalakshmi *et al*., "Smart grid technologies: communication technologies and standards," *International Journal of Applied Engineering Research*, vol. 10, no. 20, pp. 16932-16941, Nov. 2015.

[12] J. P. S. Sundaram, W. Du, and Z. Zhao, "A survey on LoRa networking: research problems, current solutions, and open issues," *IEEE Communications Surveys and Tutorials*, vol. 22, no. 1, pp. 371-388, Feb. 2020.

[13] G. Zubi, R. Dufo-López, M. Carvalho *et al*., "The lithium-ion battery: state of the art and future perspectives," *Renewable and Sustainable Energy Reviews*, vol. 89, pp. 292-308, Jun. 2018.

[14] C.-M. Tseng, C.-K. Chau, K. Elbassioni *et al*. (2021, Sept.). Autonomous recharging and flight mission planning for battery-operated autonomous drones. [Online]. Available: http://arxiv.org/abs/1703.10049

[15] M. Popa, "Smart meters reading through power line communications," *Journal of Next Generation Information Technology*, vol. 2, no. 3, pp. 92-100, Feb. 2011.

[16] K. Ashna and S. N. George, "GSM based automatic energy meter reading system with instant billing," in *Proceedings of 2013 International Mutli-conference on Automation, Computing, Communication, Control and Compressed Sensing (iMac4s)*, Kottayam, India, Mar. 2013, pp. 65-71.

[17] N. N. Doppala and A. Chavan, "Implementation of master-slave communication for smart meter using 6LOWPAN," *Advances in Decision Sciences, Image Processing, Security and Computer Vision*, vol. 4, pp. 112-118, Jul. 2019.

[18] J. Zhu and R. Pecen, "A novel automatic utility data collection system using IEEE 802. 15. 4-compliant wireless mesh networks," in *Proceedings of the 2008 IAJC-IJME International Conference*, Nashville, USA, Nov. 2008, pp. 1-10.

[19] Q. I. N. Yang and S. Yoo, "Optimal UAV path planning: sensing data acquisition over IoT sensor networks using multi-objective bio-inspired algorithms," *IEEE Access*, vol. 6, pp. 13671-13684, Mar. 2018.

[20] P. Huang, Y. Wang, K. Wang *et al*., "Differential evolution with a variable population size for deployment optimization in a UAV-assisted IoT data collection system," *IEEE Transactions on Emergency Topics and Computational Intelligence*, vol. 4, no. 3, pp. 324-335, Jun. 2020.

[21] M. Mozaffari, W. Saad, M. Bennis *et al*., "Mobile internet of things: can UAVs provide an energy-efficient mobile architecture?" in *Proceedings of the 2016 IEEE Globecom Conference*, Washington DC, USA, Dec. 2016, pp. 1-6.

[22] T. Feng, L. Xie, J. Yao *et al*., "Outage probability minimization for UAV-enabled data collection with distributed beamforming," in *Proceedings of the 2020 IEEE International Conference on Communications Workshops (ICC Workshops)*, Dublin, Ireland, Jun. 2020, pp. 1-6.

[23] R. Ilídio and M. A. Nascimento, "On best drone tour plans for data collection in wireless sensor network," in *Proceedings of the 31st Annual ACM Symposium on Applied Computing*, Pisa, Italy, Apr. 2016, pp. 703-708.

[24] C. Zhan and Y. Zeng, "Completion time minimization for multi-UAV-enabled data collection," *IEEE Transactions on Wireless Communications*, vol. 18, no. 10, pp. 4859-4872, Jul. 2019.

[25] J. Gong, T. Chang, C. Shen *et al*., "Flight time minimization of UAV for data collection over wireless sensor networks," *IEEE Journal of Selected Areas Communication*, vol. 36, no. 9, pp. 1942-1954, Sept. 2018.

[26] C. Zhan, Y. Zeng, and R. Zhang, "Energy-efficient data collection in UAV enabled wireless sensor network," *IEEE Wireless Communication Letters*, vol. 7, no. 3, pp. 328-331, Jun. 2018.

[27] C. Zhan and Y. Zeng, "Aerial-ground cost tradeoff for multi-UAV-enabled data collection in wireless sensor networks," *IEEE Transactions on Communication*, vol. 68, no. 3, pp. 1937-1950, Mar. 2020.

[28] J. Zhang, Y. Zeng, and R. Zhang, "Multi-antenna UAV data harvesting: joint trajectory and communication optimization," *Journal of Communications and Information Networks*, vol. 5, pp. 86-99, Mar. 2020.

[29] D. Zorbas and B. O'Flynn, "Collision-free sensor data collection using LoRaWAN and drones," in *Proceedings of the 2018 Global Information Infrastructure and Networking Symposium (GIIS)*, Thessaloniki, Greece, Oct. 2018, pp. 4-8.

[30] J. R. T. Neto, A. Boukercheb, R. S. Yokoyamac *et al.*, "Performance evaluation of unmanned aerial vehicles in automatic power meter readings," *Ad Hoc Networks*, vol. 60, pp. 11-25, May 2017.

[31] J. Neto, R. Yokoyana, and L. Villas, "A robust and lightweight protocol for efficient and scalable automatic meter reading using an unmanned aerial vehicle," *IEEE Latin America Transaction*, vol. 13, no. 9, pp. 3044-3050, Sept. 2015.

[32] G. Tuna, "Design considerations of UAV-aided automated meter reading," *Electrical Review*, vol. 88, no. 11, pp. 253-257, Nov. 2012.

[33] G. Tuna, "Performance evaluations on UAV-aided automated meter reading," *International Journal of Advanced Robotic Systems*, vol. 9, pp. 1-11, Sept. 2012.

[34] J. T. Neto, D. L. Guidoni, and L. Villas, "A new solution to perform automatic meter reading using unmanned aerial vehicle," in *Proceedings of the 2014 IEEE 13th International Symposium on Network Computing and Applications*, Cambridge, USA, Aug. 2014, pp. 171-174.

[35] A. Mahmood, N. Javaid, and S. Razzaq, "A review of wireless communications for smart grid," *Renewable and Sustainable Energy Reviews*, vol. 41, pp. 248-260, Jan. 2015.

[36] H. Ghazzai, A. Khattab, and Y. Massoud, "Mobility and energy aware data routing for UAV-assisted VANETs," in *Proceedings of the 2019 IEEE International Conference on Vehicular Electronics and Safety (ICVES2019)*, Cairo, Egypt, Sept. 2019, pp. 1-6.

[37] G. Masters, *Renewable and Efficient Electric Power Systems*. New Jersey: Wiley, 2013.

[38] M. Muñoz and E. Martínez, *Introduction to Batteries*. New York: Springer, 2018.

[39] I. Djurek, A. Petosic, S. Grubesa *et al*., "Analysis of a quadcopter's acoustic signature in different flight regimes," *IEEE Access*, vol. 8, pp. 10662-10670, Jan. 2020.

[40] J. Gupta, "A search algorithm for the traveling salesman problem," *Computers and Operations Research*, vol. 5, no. 4, pp. 243-250, Apr. 1978.

[41] W. Khawaja, I. Guvenc, D. Matolak *et al*., "A survey of air-to-ground propagation channel modeling for unmanned aerial vehicles," *IEEE Communications Surveys & Tutorials*, vol. 21, no. 3, pp. 2361-2391, Mar. 2019.

[42] Meter Data Collection Services. (2019, May). Kilowaze class 200 ANSI smart meter. [Online]. Available: http://meterdcs.com/wp-content/uploads/2019/09/kilowaze-ansi-meter-prod-brief-v.07-1.pdf.

[43] G. Ren, G. Ma, and N. Cong, "Review of electrical energy storage system for vehicular applications," *Renewable and Sustainable Energy Reviews*, vol. 41, pp. 225-236, Jan. 2015.

[44] Y. Salman and H. Ong, "The effect of GA parameters on the performance of GA-based QoS routing algorithm," in *Proceedings of the 2008 International Symposium on Information Technology*, Kuala Lumpur, Malaysia, Aug. 2008, pp. 1-7.

[45] A. Alajmi and J. Wright, "Selecting the most efficient genetic algo-

rithm sets in solving unconstrained building optimization problem," *International Journal of Sustainable Built Environment*, vol. 3, no. 1, pp. 18-26, Jun. 2014.
[46] A. Hassanat, K. Almohammadi, E. Alkafaween *et al*., "Choosing mutation and crossover ratios for genetic algorithms–a review with a new dynamic approach," *Information*, vol. 10, pp. 1-36, Oct. 2019.

Haiam Shahin received the B. Sc. degree in electronics and communications engineering from Mansoura University, Mansoura, Egypt, in 2008, the M. Sc. degree in electronics and communications engineering from Cairo University, Cairo, Egypt, in 2021. She worked as a Teaching Assistant in the Egyptian Russian University, Cairo, Egypt, from 2011 till 2016. She is currently working as a Lecturer in the Arab Academy for Science, Technology and Marine Transportation, Khorfakkan Branch, Khorfakkan, The United Arab Emirates. Her research interests include network and wireless communications.

Mostafa F. Shaaban received the B.Sc. and M.Sc. degrees in electrical engineering from Ain Shams University, Cairo, Egypt, in 2004 and 2008, respectively, and the Ph.D. degree in electrical engineering from the University of Waterloo, Waterloo, Canada, in 2014. He is currently an Associate Professor with the Department of Electrical Engineering, American University of Sharjah, Sharjah, United Arab Emirates, and an Adjunct with the University of Waterloo. He has several publications in international journals and conferences. He serves as an Associate Editor for IET Smart Grid and a reviewer for several refereed journals. His research interests include smart grid, renewable distributed generation, distribution system planning, electric vehicles, storage systems, and bulk power system reliability.

Mahmoud H. Ismail received the B. Sc. degree (with highest honors) in electronics and electrical communications engineering, the M. Sc. degree in communications engineering both from Cairo University, Cairo, Egypt, in 2000 and 2002, respectively, and the Ph.D. degree in electrical engineering from The University of Mississippi, Oxford, USA, in 2006. From August 2000 to August 2002, he was a Research and Teaching Assistant in the Department of Electronics and Electrical Communications Engineering at Cairo University. From 2004 to 2006, he was a Research Assistant in the Center for Wireless Communications (CWC) at the University of Mississippi. He is currently a Full Professor at the American University of Sharjah, Sharjah, United Arab Emirates, and a Full Professor (on leave) at the Department of Electronics and Electrical Communications Engineering, Cairo University. He was also a System Engineering Consultant at Newport Media Inc. (now part of Microchip) in Cairo, Egypt, from 2006-2014. He is the recipient of the University of Mississippi Summer Assistantship Award in 2004 and 2005, The University of Mississippi Dissertation Fellowship Award in 2006, The University of Mississippi Graduate Achievement Award in Electrical Engineering in 2006 and the Best Paper Award presented at the 10th IEEE Symposium on Computers and Communications (ISCC 2005), La Manga del Mar Menor, Spain. His research interests include general area of wireless communication with emphasis on performance evaluation of next-generation wireless system, coexistence, vehicular network, and communications over fading channel.

Hebat-Allah M. Mourad received the B.Sc., M.Sc. and Ph.D. degrees in electrical communication engineering from Cairo University, Cairo, Egypt, in 1983, 1987, and 1994, respectively. Since 1983, she has been with the Department of Electronics and Electrical Communications, Faculty of Engineering, Cairo University, and is currently a Professor there. She was the Director of high technology center, Faculty of engineering, Cairo university from 2008 till 2012. She was a Member of the technical office of the post graduate and research sector of Cairo university from 2010 till 2012. She is named in Marquis Who's Who in Science and engineering in the year 2004. Her research interests include wireless and mobile communications.

Ahmed Khattab received the B.Sc. (honors), M.Sc. degrees in electrical engineering from Cairo University, Cairo, Egypt, in 2004 and 2002, respectively, the master of electrical engineering degree from Rice University, Huston, USA, in 2009, and the Ph.D. degree in computer engineering from the Center for Advanced Computer Studies (CACS) at the University of Louisiana at Lafayette, Lafayette, USA, in 2011. He is an Associate Professor in the Electronics and Electrical Communications Engineering Department at Cairo University that he joined in 2012 as an Assistant Professor. He authored/co-authored 3 books, 4 book chapters, over 100 journal and conference publications, and a U.S. patent. Dr. Khattab is the recipient of Egypt State First Class Medallion of Excellence in 2020 and Egypt State Encouragement Award for Engineering Sciences in 2017. He has also won several awards from different IEEE conferences and sociaties. His current research interests include Internet of Things, wireless sensor network, vehicular network, cognitive radio network, security, and machine learning.